phys. stat. sol. (c) **5**, No. 6, 1655–1658 (2008) / **DOI** 10.1002/pssc.200778571

physica status solidi c
www.pss-c.com
current topics in solid state physics

X-ray diffraction studies of selective area grown InGaN/GaN multiple quantum wells on multi-facet GaN ridges

S. M. O'Malley[*,1], P. L. Bonanno[1], T. Wunderer[2], P. Brückner[2], B. Neubert[2], F. Scholz[2], A. Kazimirov[3], and A. A. Sirenko[1]

[1] Department of Physics, New Jersey Institute of Technology, Newark, NJ 07102, USA
[2] Institute of Optoelectronics, Ulm University, 89081 Ulm, Germany
[3] Cornell High Energy Synchrotron Source (CHESS), Cornell University, Ithaca, NY 14853, USA

Received 7 September 2007, revised 3 December 2007, accepted 26 December 2007
Published online 17 April 2008

PACS 61.05.cp, 68.65.Fg, 81.05.Ea, 81.07.St, 81.15.Kk

[*] Corresponding author: e-mail so26@njit.edu, Phone: 973 596 5879, Fax: 973 596 5794

The structural properties of InGaN/GaN multiple quantum wells (MQW) were studied using synchrotron based high resolution x-ray diffraction (HRXRD). MQW structures were grown on the top and sidewall facets of triangular and trapezoidal shaped GaN ridges by metalorganic vapour phase epitaxy (MOVPE) in the regime of selective area growth (SAG). Period and strain variations as a function of oxide mask width were determined for both the sidewall and the top facet growth. Oxide mask widths ranged between 2 and 20 μm with openings between adjacent masks of 4 and 6 μm. Analysis of the x-ray diffraction curves revealed a sidewall / vertical growth rate ratio of ~0.3 through a comparison of the top to sidewall facet MQW periods. Masks orientated along the <11-20> crystallographic direction showed stronger growth enhancement along with large global strain for MQW growth on the top (0001) plane. Interpreting our results within the framework of vapour phase diffusion revealed that inter-facet migration of group-III species needs to be taken into account.

1 Introduction The optical efficiency of InGaN quantum well (QW) devices is hindered by the presence of large piezoelectric fields within the active region [1]. One way to reduce this problem is to grow QWs on semi-polar planes instead of the commonly used (0001) *c*-plane [2]. The epitaxial growth of GaN between dielectric masks patterned on the substrate surface, in a process known as selective-area-growth (SAG), forms GaN ridges with semi polar sidewall facets. These sidewall facets provide an ideal plane for the subsequent growth of QW structures [3]. Currently, most groups have relied on imaging techniques to examine the relationship between top and sidewall facet growth. However, such techniques only provide limited information on the structural parameters in the active region.

In this paper, synchrotron radiation based high resolution x-ray diffraction (HRXRD) was used to examine the influence of mask width and orientation on the period and strain of InGaN/GaN MQW growth on both top and sidewall facet planes. Results extracted from the diffraction curves were interpreted within the framework of vapor phase diffusion and surface migration effects. The goal of these studies is to gain a better understanding of the growth dynamics involved in the SAG fabrication of GaN-based devices with various mask parameters e.g. width and orientation.

2 Experimental Samples were grown by low-pressure MOVPE in a single-wafer Aixtron system with a horizontal reactor design. A GaN buffer layer was grown epitaxially on c-plane sapphire (Al_2O_3) substrates. The dielectric mask pattern was created by growth of an oxide layer of SiO_2 (200 nm thick) on the GaN buffer layer by PECVD and patterned by optical lithography and reactive ion etching. Then, n-doped GaN ridges where grown inside the unmasked regions with growth conditions optimized for triangular/trapezoidal shaped ridges. The MQW structure was then grown on the GaN ridge structures, consist-

ing of five InGaN quantum wells separated by GaN barriers. Lastly, the device structure was finished with a p-doped GaN:Mg capping layer with a target thickness of ~0.2 µm. Two mask orientations were chosen: sample S1 had masks oriented parallel to the <11-20> crystallographic direction and sample S2 along the <1-100> direction. The ridge sidewall facets depend on mask direction, thus, S1 has {1-101} sidewall facets and S2 {11-22} sidewall facets. Mask design was selected to produce arrays of identical GaN ridges, where the mask width A varies from A = 2 to 20 µm in 2 µm steps, and the unmasked width B is fixed to either B = 4 or 6 µm. Sample growth details and results of SEM and optical characterization are described in details in Ref. [3]. Preliminary data for x-ray diffraction studies of S1 using microbeam synchrotron radiation are described in Ref. [4].

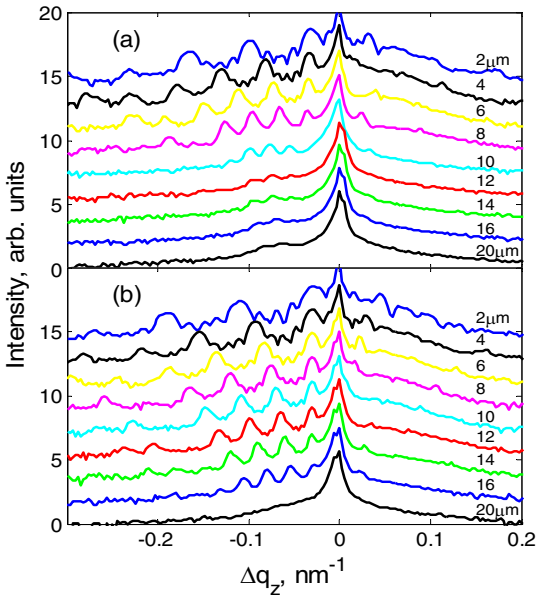

Figure 1 θ-2θ scans for symmetric (00.2) reflections from samples S1 (a) and S2 (b) for 6 µm wide openings with mask width A varied from 2 µm (upper curve) to 20 µm (lowest curve). Intensity shown in log scale and horizontal axis is presented in relative reciprocal lattice units (q_z [00.2] = 3.863 nm^{-1}). Diffraction curves are vertically offset for clarity.

High-resolution x-ray diffraction (HRXRD) was performed at the A2 beamline of Cornell High Energy synchrotron Source (CHESS). The incident synchrotron beam was initially conditioned to an energy of E = 10.531 keV. The samples were mounted in a four-circle Huber diffractometer, with ridges oriented along the diffraction plane. The scattered beam was then conditioned by a single bounce Si (111) analyzer crystal and finally collected by a Bede scintillation detector. A pair of orthogonal slits positioned before the sample determined the beam size, 0.2 × 0.2 mm^2, incident on the sample surface. This allowed several identical ridges within a particular array to be probed simultaneously. The sidewall facet grown MQW, were probed by rotating the sample about an angle chi (χ), thus bringing the sidewall MQW perpendicular to the diffraction plane, thereby enabling coplanar θ-2θ scans. Sample S1 with its {1-101} sidewall facets was rotated to χ = 61.9 deg, while S2 {11-22} was rotated to χ = 58.4 deg.

3 Results and discussion Measurements of θ-2θ scans were carried out systematically for both samples by varying the mask and opening width. The symmetric (00.2) reflection was used to probe MQW growth on the top of the GaN ridges. Bragg condition for GaN was satisfied at $\theta_{00.2}$ (GaN) = 13.142 deg., which corresponds to q_z = 3.863 nm^{-1}. Figure 1 depicts the θ-2θ diffraction scans from the 6 µm wide mask opening of samples S1 and S2. Superlattice (SL) peaks associated with the presence of a MQW structure grown on the top (00.1) plane can clearly be seen for both mask orientations. Interstitial *N-2* Kiessig fringes (maxima) are visible for narrow mask widths, attesting to the high angular resolution of the setup with effective suppression of the diffused background. The SL peak intensity diminishes noticeably with increased mask width in both samples. However, S2 retains its peak visibility up to A = 16 µm, with its mask orientated along the <1-100> direction. Scans from S1 with 4 µm ridges showed only the GaN substrate peak; no visible SL peaks were present. Sample S2, however, did have SL peaks, visible up to the maximum 20 µm wide oxide mask width. Sidewall growth was examined using the (20.2) reflection from {1-101} sidewall facets of S1 and the (11.2) reflection from {11-22} facets of S2. In both samples, sidewall SL peaks are present for the narrower 4 µm wide ridges. (Note: neither 4 µm ridges nor sidewall diffraction curves shown.)

MQW periods were determined by measuring separation between adjacent SL peaks. Figure 2a compares the periods of samples S1 and S2 at various mask widths for the top (0001) planar growth from 6 µm wide ridges. Sample S1 shows a linear increase with mask width until the onset of saturation for A > 8 µm. Sample S2, periods displayed linear dependence for almost the entire range, deviating only slightly at the largest mask widths. The solid line in Fig. 2a represents the expected growth enhancement for the period thickness according to the law of conservation of source material in periodic arrays: $P = P_0(A+B)/B$, where P_0 is the layer thickness for unmasked growth, A is the mask width and B is the opening. Strain S was determined by the separation between the 0th order MQW peak and the GaN substrate peak. Values of S are presented in the units of the d-spacing mismatch. Strain and indium composition analysis for MQWs was carried out using BEDE software for simulation of diffraction curves using dynamic diffraction theory [4]. We assumed elastic strain between MQW and GaN substrate, which has been confirmed by asymmetric reciprocal space mapping (results will be published elsewhere). Strain for S1 6 µm ridges (Fig. 2b) increased linearly, from S = 0.82% to 0.91%, with

mask width, while S2 only ranged from S = 0.73% to 0.76 % though within a larger mask width range (A = 2 to 14 µm).

Variation of the MQW period for top and sidewall growth is shown in Fig. 2c for both the 4 and 6 µm wide ridges from sample S2. Comparison between the top and sidewall growth reveals a lateral / vertical growth rate ratio of ~0.3. In Fig. 2c, growth enhancement is stronger for the narrower 4 µm opening with an earlier onset of saturation. The global MQW strain values for the 4 µm ridges from S2 were S ~ 0.78 % and 0.59, for top and sidewalls growth, respectively, which corresponds to an approximate 24% reduction in strain for the sidewall grown MQW structure. Figure 2d compares sidewall periods for samples S1 and S2 with a 4 µm openings.

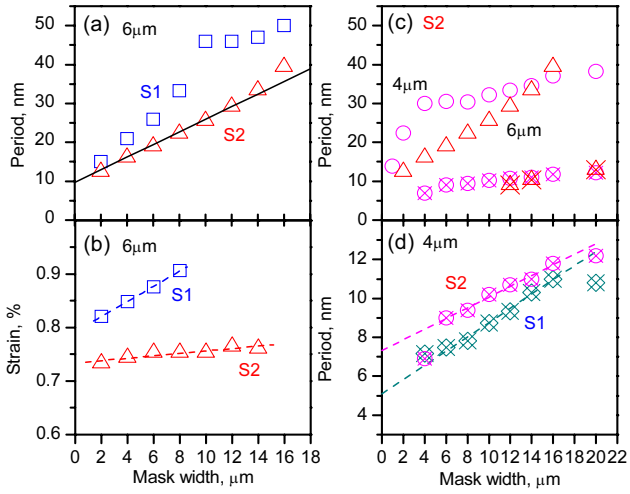

Figure 2 (a) MQW period vs. mask width A, for S1 (box) and S2 (triangle) 6 µm wide ridges. Solid line represents fit to growth rate enhancement model. (b) Global MQW strain for S1 and S2, determined from the (00.2) reflection. (c) MQW period vs. mask width, for top (symbol) and sidewall (symbol+cross) MQW from S2. (d) Period comparison between sidewall grown MQW from S1 and S2 with 4 µm opening. Dashed lines represent regression line fit.

When comparing MQW periods between the two mask orientations (Fig. 2a, 2d), the larger slopes for S1 indicates stronger growth rate enhancement with its <11-20> orientated mask than S2 with <1-100> mask orientation. The common interpolated intersect at A = 0 reinforces the fact that both samples were grown under the same reactor conditions. Growth enhancement for samples with identical mask pattern and reactor conditions ought to have similar structural parameters under the law of source material conservation based on the gas phase diffusion of precursors towards the growth surface. Therefore, results in Fig. 2, which clearly highlight the difference in strain and growth enhancement, indicate that other considerations must be taken into account, such as the exact ridge dimensions and inter-facet migration of group-III species. Relating ridge profile evolution obtained by SEM to the MQW period dependence observed in Fig. 2a suggests that S1 B = 6 µm experiences a "shape transition" with increasing mask width, from a trapezoidal to triangular shape at A ~ 8 µm. The diminishing visibility of MQW satellite peaks with increased mask width and a static MQW period for $A \geq 10$ µm corresponds to termination of the sidewall growth at the apex of triangularly shaped ridges. The 6 µm wide ridges of S2 do not experience a full evolution to a triangular profile and therefore do not experience saturation in growth enhancement. The conservation of source material equation used to model the growth enhancement assumes an ideal rectangular ridge profile. Therefore, the top ridge width (b) should be identical to the opening width (B). However, SEM images revealed that b is in fact less then B. The smaller ridge tops should then experience significantly larger growth enhancement than that predicted using B in the model. Further complicating matters is the overgrowth experienced in the SAG of GaN. This overgrowth, commonly referred as "wings," reduces the masked width A [4]. In spite of these discrepancies, there is surprisingly good agreement between the growth enhancement model and actual experimental data for the S2 6 µm width ridges. The sidewall facet growth may have contributed to this agreement by reducing the overall concentration of group-III precursors over the ridge tops.

Fitting the θ-2θ scans for top ridge growth using commercially available RADS Mercury Bede software produced an indium concentration of 12.5% for S1 and 11.5% for S2; these values were independent of mask width. The fitting, using the dynamic theory of x-ray diffraction, allowed for decoupling of the well and barrier thicknesses [5]. This revealed that InGaN wells in S1 grow faster than the GaN barriers. The global MQW strain in S1, which increases with mask width, is due to the larger well growth rate. Sample S2 growth rates for well and barrier were fairly similar, explaining the samples relatively constant strain dependence. The difference in growth rates, and subsequently the strain dependence found between the samples, may be due to inter-facet migration effects, where indium can migrate further on the {1-101} sidewall facet of S1 and contribute to growth on the top (0001) ridge plane.

4 Conclusion We discerned that the gas-phase diffusion model can qualitatively predict the top facet grown MQW period dependence on mask width from 2 to 16 µm for all but the narrowest ridges, where short range inter-facet migration effects of the group-III reactants need to be taken into account. More detailed studies of this effect based on a combination of SEM and microbeam HRXRD results will be published elsewhere.

References

[1] F. Bernardini, V. Fiorentini, and D. Vanderbilt, Phys. Rev. B **56**, R10024 (1997).

[2] T. Takeuchi, H. Amano, and I. Akasaki, Jpn. J. Appl. Phys., Part 1 **39**, 413 (2000).

[3] B. Neubert, P. Brückner, F. Habel, F. Scholz, T. Riemann, J. Christen, M. Beer, and J. Zweck, Appl. Phys. Lett. **87**, 182111 (2005).
[4] A. A. Sirenko, A. Kazimirov, S. Cornaby, D. H. Bilderback, B. Neubert, P. Brückner, F. Scholz, V. Shneidman, and A. Ougazzaden, Appl. Phys. Lett. **89**, 181926 (2006).
[5] A. A. Sirenko, A. Kazimirov, A. Ougazzaden, S. M. O'Malley, D. H. Bilderback, Z.-H. Cai, B. Lai, R. Huang, V. K. Gupta, M. Chien, and S. N. G. Chu, Appl. Phys. Lett. **88**, 081111 (2006).

